

# Improving Deep Learning for Seizure Detection using GAN with Cramer Distance and a Temporal-Spatial-Frequency Loss Function

Indurani Palanichamy<sup>1</sup>, Dr. Veni Sundaram<sup>2</sup>

<sup>1</sup>Department of Computer Science  
Karpagam Academy of Higher Education  
Coimbatore, India  
induppsphd16@gmail.com

<sup>2</sup>Department of Computer Science  
Karpagam Academy of Higher Education  
Coimbatore, India  
venics@kahedu.edu.in

**Abstract**— The signals of EEG are analyzed in the identification of seizure and diagnosis of epilepsy. The visual examination process of EEG data by skilled physician is huge time-utilization and the judgemental process is complicated, which may vary or show inconsistency among the physician. Hence, an automatic process in diagnosis and detection was initiated by the Deep Learning (DL) approaches. Time Aware Convolutional Neural Network with Recurrent Neural Network (TA-CNN-RNN) was one among them. Deep neural networks trained on large labels performed well on many supervised learning tasks. Creating such massive databases takes time, resources, and effort. In many circumstances, such resources are unavailable, restricting DL adoption and use. In this manuscript, Generative Adversarial Networks with the Cramer distance (CGAN) is proposed to generate an accurate data for each lable. A spatiotemporal error factor is introduced to differentiate actual and genetrated data. The discriminator is learned to differentiate the created data from the actual ones, while the generator is learned to create counterfeit data, which are not estimated as false by the discriminator. The classical GANs have a complex learning because of the nonlinear and non-stationary features of EEG data which is solved by Carmer Distance in the proposed method. Finally, the sample generated by CGAN is given as input for the Time Aware Convolutional Neural Network with Recurrent Neural Network (TA-CNN-RNN) classifier to investigate experimental seizure Prediction outcome of the proposed CGAN. From the investigational outcomes, the proposed CGAN- TA-CNN-RNN model attained classification accuracy of 94.6%, 94.8% and 95.2% on CHB-MIT-EEG, Bonn-iEEG and VIRGO-EEG than other existing EEG classification schemes and also provides great potentials in real-time applications.

**Keywords**- Seizure, epilepsy, Cramer distance, electroencephalogram, LSTM detection and diagnosis.

## I. INTRODUCTION

An epileptic seizure is a momentary incidence of signs because of the exciting or asymmetrical activities of neurons in the brain [1]. Generally, the incidence of epilepsy in the brain is confirmed and examined by the visual investigation of long-term of recorded scalp electroencephalograms (EEGs) and it spots the existence of epileptic seizure that utilises vast time to process or to identify the epilepsy[2]. Automated diagnosis system finds the epileptic seizure significantly reduces the duration of process of diagnosis [3][4].

Numerous features are encompassed for the automatic detection or diagnosis of seizure in the brain. The values or features from EEG utilized in the automatic detection of seizure that is the connectivity of autocorrelation, functional network properties, EEG's morphology, likelihood calculations and nearest neighbour [5], [6]. The early diagnosis of seizure is a

indispensable to cure the disease [7]. The repeated features in the domain of EEG are detected via the rhythmic actions that are frequently monitored in the seizures [8]. The existence of seizure in brain can be identified from the features of the EEG signals. The features are easily identifiable that are statistical, spectral, nonlinear features, and principal components [9]-[10].

The features from the signals have depicted excellence in the detection of definite variety of seizure [11]-[13]. The diversified nature of seizure made several difficulties to develop a global feature for the automation in the seizure recognition [14]. Additionally, the seizures in the brain are infrequently happening event and it is appropriate in training the problematical process of the supervised learning of seizure with the linear variety of Machine Learning (ML) classifiers, support vector machine (SVM), artificial neural network (ANN), and other computational models [15]-[17]. However, in traditional ML methods, feature and classifier selection is performed by a trial-

and-error approach [18]. As the quantity of available data has grown in recent years, the effectiveness of ML methods may have decreased.

DL methods have been incorporated into all disease detection applications because of its superior signal and images representation [19]. In several areas of medicine, including the identification of epileptic seizures, such methods have led to significant advancements [20]. Considerable effort has been put into developing DL models for epilepsy detection including convolutional neural networks (CNNs), recurrent neural networks (RNNs), deep belief networks (DBNs), Autoencoders (AEs), and CNN-RNNs and CNN-AEs [21]–[23]. As more and more effective models for the early identification of epileptic seizures are proposed, the number of DL-based studies in this field has increased. For instances, the CNN based epileptic seizures detection models can correctly recognized irregular inter-ictal discharges as non-seizures, but could not detect the ictal state and slower oscillations [24]. To improve the performance of CNN for detecting seizures ictal state and slower oscillations, Recurrent Neural Network (RNN) is combined with CNN model. The seizure detection at the early stage is necessary and it is significant to detect with the computational algorithms.

For the efficient epileptic seizure detection, Time-aware CNN with RNN (TA-CNN-RNN) was proposed to extract features from signals for different time and frequency [25]. TA-CNN-RNN was incorporated with the position information into CNN via an attention mechanism. LSTM is used as RNN in this work. The training epoch used in the RNN greatly reduces the number of training-phase errors, which in turn boosts the RNN's accuracy. TA-CNN-RNN demonstrated the capability to deliver notable efficiencies on a widespread variety of supervised training processes if learned on widespread gathering of labeled samples. However, TA-CNN-RNN required the vast amount of relevant information in datasets.

In order to overcome the issues of collecting large annotated datasets, Generative Adversarial Networks along the Cramer distance (CGAN) is integrated to reduce the amount of labeled data required for identification tasks. In this model, GAN [26] is adopted to generate required labelled data. The discriminator is learned to differentiate the created data from the actual ones, while the generator is learned to create counterfeit data, which are not estimated as false by the discriminator. During EEG data creation, GANs have a complex learning because of the nonlinear and non-stationary features of EEG data. To combat this issue, Cramer Distance [27] is used to compare sample distribution. The Cramer Distance is the alternative solution to Wasserstein metric which effectively leverages effective probabilistic forecasting results. The Cramer Distance is applied on the GANs model to provide more stable learning and increased diversity in the generated samples. Finally, the

generated dataset by CGAN is given as input to TA-CNN-RNN classifier for the efficient prediction of seizure from EEG signals for epilepsy disease.

The rest of the sections are emphasised as follows, previous works and literature is described in the Section 2, the detection and diagnosis of epilepsy in the EEG signal is attained by the proposed DL approach is detailed in Section 3, the numerical outcome of the experiment is provided in Section 4 and the proposed TA-CNN-RNN model is concluded with future suggestion.

## II. RELATED WORKS

The EEG brain signals are utilised for the identification of epilepsy with the DL techniques. An ensemble approach of pyramidal one dimensional convolutional neural network (P-1-D-CNN) was utilized in the identification epileptic disorder. The approach was not effective when it uses huge number of learning parameters [28]. The scalogram based CNN (SCNN) was utilised for the identification of five class EEG records [29]. The Self-Aware Distributed ML model [30] was designed, which allocates the complicated and ER-consumed machine learning algorithm from edge to cloud according to the idea of self-consciousness for epilepsy identification in the real world.

The epilepsy was identified by the wavelet based DL technique whereas ternary and binary classification were accomplished with this approach. The DL process eliminates the extraction of features and directly classifies the epilepsy [31]. Additionally, associate petri net and fuzzy entropy was incorporated with wavelet-based EEG processing. This approach was effective in the identification of epilepsy. The negative predication may lead to the misclassification [32]. Time-Frequency Localised Bi-orthogonal Wavelet Filter was used for the classification and the classification is attained for diversified classes [33].

The shortcomings in the existing systems are considered and rectified in this paper. The necessity of huge semi-supervised learning technique and annotated datasets is assimilated to deep learner to minimize the quantity of labeled sample needed via adopting GAN with Cramer distance and a spatiotemporal error factor for a DL setting.

The rest of the sections are emphasized as follows, previous works and literature is described in the Section 2, the detection and diagnosis of epilepsy in the EEG signal is attained by the proposed deep learning approach is detailed in Section 3, the numerical outcome of the experiment is provided in Section 4 and the proposed TA-CNN-RNN model is concluded with future suggestion

### III. IMPROVING SEIZURE PREDICTION USING CGAN

In this research, a new regeneration method is developed depending on the CGAN and a spatiotemporal error factor. The spatiotemporal error factor regenerates data through determining the Mean Square Error (MSE) from time-series attributes, general spatial attributes and power spectral density attributes. The GAN encompasses a generator and a discriminator, which are fine-tuned to reduce the 2-player min-max issue. The discriminator is learned to differentiate the produced data from the actual data, whereas the generator is learned to create counterfeit data, which are not estimated as false by the discriminator while generating EEG data, GANs have a difficult learning because of the nonlinear and non-stationary attributes of EEG data. To resolve this challenge, Cramer Distance is used to compare sample distribution Fig. 2 shows the proposed model.

#### A. Re-Construction of EEG Signals

For the EEG signal reconstruction, the EEG signal in LSS is denoted as  $z \in S^{N \times TS_1 \times R}$  that is from the distribution of signal  $D_L$  and the EEG signal in HSS is denoted as  $x \in S^{N \times TS_2 \times R}$  that is from the distribution of signal  $D_H$ . In the description, the count of the channel is signified as  $N$ . The LSS-EEG signal's samples of trial and HSS-EEG signal's samples of trial is denoted as  $TS_1$  and  $TS_2$ , respectively. The motor-based task and their count is denoted as  $R$ . The main intent of reconstruction is to devise an operation  $fn(z)$  which denote

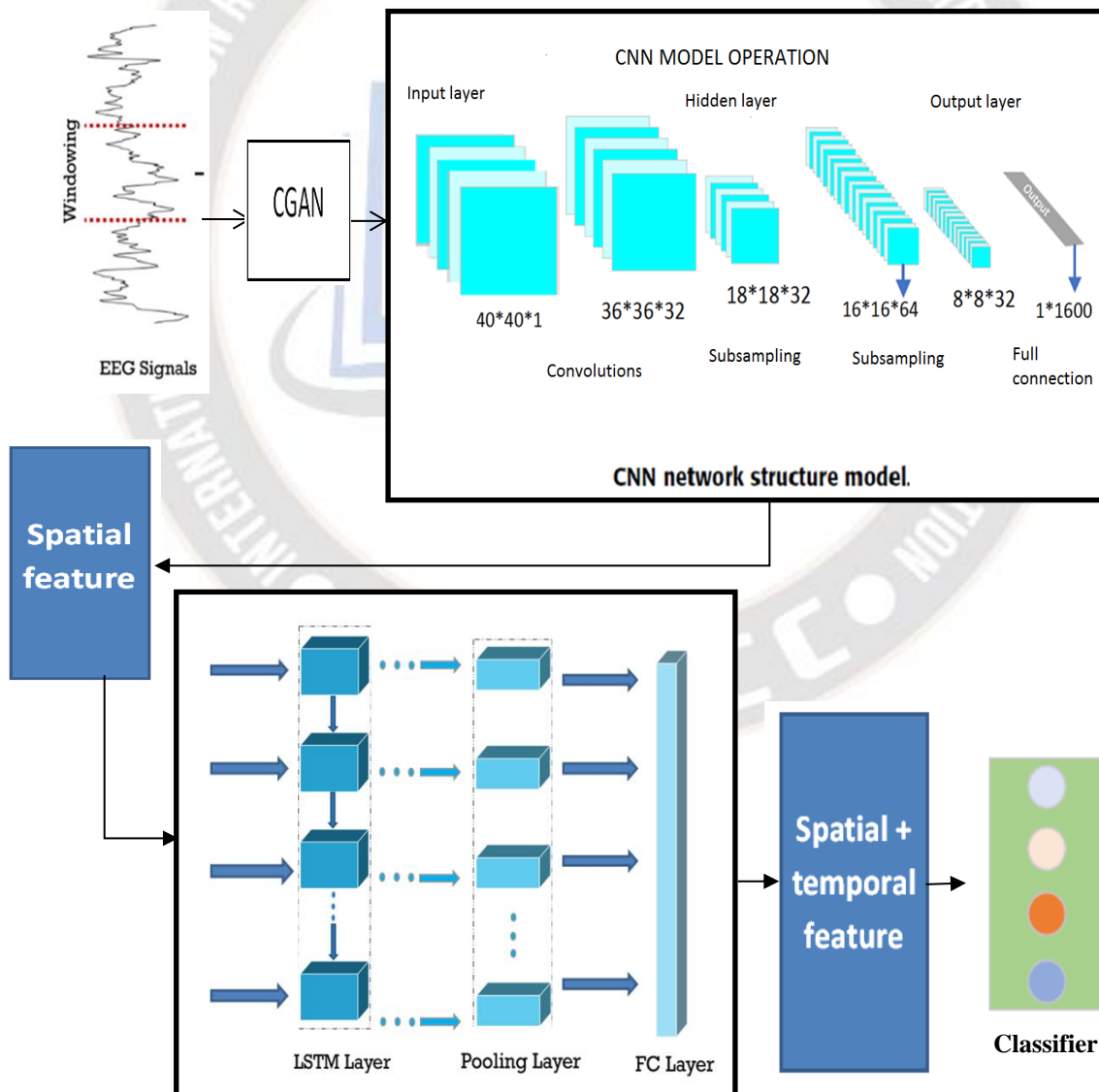


Figure 1. Framework for Epilepsy detection using CGAN-TA-CNN-RNN

$$fn(z): z \rightarrow x \tag{1}$$

the  $z$  as LSS-EEG signal and  $x$  as HSS-EEG signal as Eq. (1). During a process of regeneration, the attribute maps the samples of LSS-EEG from  $D_L$  into  $D_C$  that is particular distribution and the aim is altering a particular distribution that is near to the actual distribution  $D_H$  via deviating  $fn(z)$ . The process of regeneration encompasses 2 methods. During the process of creation, the data alters EEG information from  $D_L$  to the  $D_C$ . The process of reconstruction of EEG is treated as the alteration procedure of EEG from a distribution to the other distribution.

Generally EEG data are non-stationary and nonlinear, the noise model in the data makes complication and non-uniformly maps the reconstruction relationship that is distributed. The distribution of HSS-EEG and LSS-EEG has no clear suggestion where the signals are correlated. The LSS-EEG reconstruction is complicated process with the traditional techniques. Conversely, the noise model's uncertainties and the relationship in reconstruction mapping are avoided by utilizing Deep Neural Networks (DNNs).

**B. GAN with Cramer Distance**

Fig. 2 depicted the overall of functionality of CGAN. Cramer distance poses the similar distance properties as Wessertein metric and it faces the drawback of sample unbiased gradient. For two EEG signal distributions,  $z \in S^{N \times TS_1 \times R}$  that is from the distribution of signal  $D_L$  and the EEG signal in HSS is denoted as  $x \in S^{N \times TS_2 \times R}$  that is from the distribution of signal  $D_H$ . The Cramer distance among the LSS and HSS is given as Eq. (2)

$$C_2^2(L, H) := \int_{-\infty}^{\infty} (D_L(x) - D_H(x))^2 dx \tag{2}$$

The square root of Cramer distance and their relevant member of the metric family  $C_p$  is given as Eq. (3)

$$C_p(L, H) := \left( \int_{-\infty}^{\infty} |D_L(x) - D_H(x)|^p dx \right)^{1/p} \tag{3}$$

The Cramer distance metric has dual forms with the integral probability and it is given as Eq. (4)

$$(L, H) = \sup_{fn \in F_q} | \int_{x \sim L} fn(x) - \int_{x \sim H} fn(x) | \tag{4}$$

Where,  $FH: = \{fn: f \text{ is generally continuous, } \left\| \frac{df}{dx} \right\|_q \leq 1\}$  where  $H$  is the conjugate exponent of  $L$  that is  $L - 1 + H1 = 1$ . It is a dual form that utilises to prove the Cramer distance.

The GAN is composed of discriminator  $DI$  and generator  $GE$ , which optimises the min-max issue in two layers. The EEG signal reconstruction is determined by discriminator ( $DI_{\theta_{DI}}$ ) and generator ( $GE_{\theta_{GE}}$ ) is given as Eq. (5)

$$\min_{\theta_{GE}} \max_{\theta_{DI}} L_{GAN}(DI_{\theta_{DI}}, GE_{\theta_{GE}}) = E_{x \sim D_H} [\log DI_{\theta_{DI}}(x)] + E_{z \sim D_L} [\log (1 - DI_{\theta_{DI}}(GE_{\theta_{GE}}(z)))] \tag{5}$$

where the expectation vector is denoted by  $E(\cdot)$ . If the  $DI$  attains the actual information, it can gratify  $DI_{\theta_{DI}}(x) = 1$  to differentiate the actual information. At this point,  $DI_{\theta_{DI}}(x) = 1$  influences the anticipation for  $\log DI_{\theta_{DI}}(x)$ . If the  $DI$  attains the created information it can gratify  $DI_{\theta_{DI}}(GE_{\theta_{GE}}(z)) = 0$  to created information that is discriminated. Here,  $DI_{\theta_{DI}}(GE_{\theta_{GE}}(z)) = 0$  attains the expectation for  $(1 - DI_{\theta_{DI}}(GE_{\theta_{GE}}(z)) = 0)$ . Consequently, the optimal function of minimax is developed using the expectation function. The common regeneration notion is to learn a  $GE$  to fool a dissimilar  $DI$ , which is learned to discriminate to reconstruct the HSS-EEG data from the actual HSS-EEG data. In building EEG data, GANs have a complex learning because of the non-stationary and nonlinear features of EEG data. To combat the issues in learning architecture of the actual GAN, rather than utilizing the Jensen–Shannon divergence, the CGAN architecture utilises

Cramer distance to compare the distribution of sample. According to the design of CGAN, the optimization of min-max issue is attained by  $DI_{\theta_{DI}}$  and  $GE_{\theta_{GE}}$ . It can be equated as Eq. (6)

$$\min_{\theta_{GE}} \max_{\theta_{DI}} L_{CGAN}(DI_{\theta_{DI}}, GE_{\theta_{GE}}) = E_{x \sim D_H} [DI_{\theta_{DI}}(x)] + E_{z \sim D_L} [DI_{\theta_{DI}}(GE_{\theta_{GE}}(z))] + \lambda E_{\tilde{x} \sim D_R} [( \|\nabla_{\tilde{x}}(D(\tilde{x}))\|_2 - 1)^2] \tag{6}$$

In the issue of min-max, the Cramer distance is calculated using the initial 2 expressions. The final expression is the gradient consequence for the normalization of the network. In the expression of penalty,  $D_R$  signifies the uniform distribution of samples  $\tilde{x}$  across straight lines joining sets of created and actual data.  $\nabla_{\tilde{x}}(\cdot)$  is the gradient estimator, and a penalty term

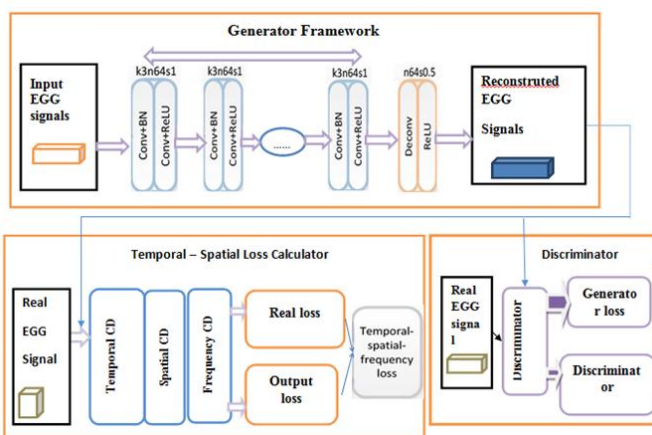


Figure 2. Frameworks CGAN

for a constant weighting parameter is signified as the parameter  $\lambda$ . In fact, the CGAN architecture eliminates drips the last sigmoid layer and the log function to maintain the gradient value during learning the min-max issue.  $DI_{\theta_{DI}}$  and  $GE_{\theta_{GE}}$  are learned optionally through fine-tuning one and upgrading another.

### C. Loss function of TSF-MSE

The transformation of the generator is permitted for the distribution of information from low to maximum sampling ratio, another portion of error factor necessitates CGAN framework. This will preserve the content information and detail of the EEG data. A broadly utilised error factor for the detail and data content is the MSE. Generally, MSE is estimated by reducing the error by pointwise in processing the signals, the temporal MSE is estimated via reducing the instance sampling of loss by pointwise among the patches of LSS-EEG and HSS-EEG using the interval is given as Eq. (7)

$$L_{T-MSE}(GE_{\theta_{GE}}) = E_{(x,y)} \left[ \frac{1}{T^2} \left\| GE(z(t)) - x(t) \right\|_p^2 \right] \quad (7)$$

In distinction with scans, EEG data are multi-channel time-series information and the spatial and spectrum attributes should be taken during regeneration. To support the GAN/CGAN design to build highly precise HSS-EEG data, the spatial MSE LS-MSE among channels and the spectrum MSE LF-MSE among data batches must also be addressed along with the temporal MSE LT-MSE across intervals.

Common Spatial Patterns (CSP) and Power Spectral Density (PSD) attributes are broadly utilised to retrieve spatial attributes and spectrum attributes from EEG data, correspondingly. The CSP techniques is utilised for determining the best projection vectors to reflect the actual EEG data to a novel space for acquiring the best spatial resolution and prejudice among diversified labels of EEG data. The PSD technique is utilised for determining the energy ranges on precise bands to comprise a spectra. Utilising such techniques, the spatial MSE  $L_{S-MSE}$  and the spectrum MSE  $L_{F-MSE}$  are determined for the GE Eq. (8), Eq. (9)

$$L_{S-MSE}(GE_{\theta_{GE}}) = E_{(x,z)} \left[ \frac{1}{C^2} \left\| GE(CSP(z(c)) - CSP(x(c))) \right\|_F^2 \right] \quad (8)$$

$$L_{F-MSE}(GE_{\theta_{GE}}) = E_{(x,z)} \left[ \frac{1}{N^2} \left\| GE(PSD(z(n)) - PSD(x(n))) \right\|_F^2 \right] \quad (9)$$

where the feature extractors of CSP and PSD are  $CSP(\cdot)$  and  $PSD(\cdot)$  correspondingly. The actual and generated EEG signal's channel is given as  $c$  and the count of the channel is  $C$ , batch of the signal is  $n$  and the count of generated signal batch is  $N$ . For

accessibility, the TSF error is calculated by weighing 3 MSEs Eq. (10)

$$L_{TSF-MSE}(G_{\theta_G}) = \lambda_T \cdot L_{S-MSE}(G_{\theta_G}) + \lambda_S \cdot L_{S-MSE}(G_{\theta_G}) + \lambda_F \cdot L_{S-MSE}(G_{\theta_G}) \quad (10)$$

where  $\lambda_T, \lambda_S, \lambda_F$  are the weights of 3 diversified MSEs, correspondingly. Additionally, the EEG data are spatially and temporally rational with a normalization error  $L_{TV}(GE_{\theta_{GE}})$  depending on overall deviation is utilised in the GEN Eq. (11)

$$L_{TV}(GE_{\theta_{GE}}) = \frac{1}{CT} \sum_{c=1}^C \sum_{t=1}^T \left\| \nabla_z GE_{\theta_{GE}}(z)_{c,t} \right\| \quad (11)$$

where the gradient estimator is signified as  $\nabla_z(\cdot)$ , the gradient normalization error can support spatial and temporal consistency of the regeneration. Fusing formulas CGAN, TSF loss and regularization loss, the total mutual regeneration error factor is given by Eq. (12)

$$\min_{\theta_{GE}} \max_{\theta_G} L_{TSF-MSE}(GE_{\theta_{GE}}) + \lambda_1 L_{CGAN}(DI_{\theta_{DI}}, GE_{\theta_{GE}}) + \lambda_2 L_{TV}(GE_{\theta_{GE}}) \quad (12)$$

Where the tradeoff of the controlling weights are indicated as  $\lambda_1$  and  $\lambda_2$  that lies between the CGAN adversarial, the TSF-MSE and the TV losses. The architecture of CGAN-EEG is trained by diverse batches of EEG signals and utilised in every single trial. The framework is trained for the effective classification of the epilepsy in the EEG signal.

## IV. RESULT AND DISCUSSION

In this section, the outcome of the epilepsy classification by the proposed and existing approach is discussed. The data in the Bern-Barcelona EEG database is collected from patients with the incidence of epilepsy that comprises non-focal and focal channels with 1024Hz. The database holds 3750 pairs of signals recorded from the channels of EEG and the recorded samples are divided into slots of windows with the interval of ten seconds, which results the sample of 10240. For this experiment, the publicly accessible EEG databases which are already used in many published articles are used. CHB-MIT Scalp EEG Database [34], Bonn iEEG dataset [35], and VIRGO EEG dataset [36] are used in this paper. The experiment is accomplished in the Matlab with the computation atmosphere's RAM 8.00 GB and CPU 2.30 GHz. The numerical outcomes of the experiment is evaluated using the performance metrics namely accuracy, precision, f-measure and recall. Fig. 3 display the EEG signal and the EEG with the incidence of epilepsy. P-1D-CNN (28), S-CNN [29] and TA-CNN-RNN [25].

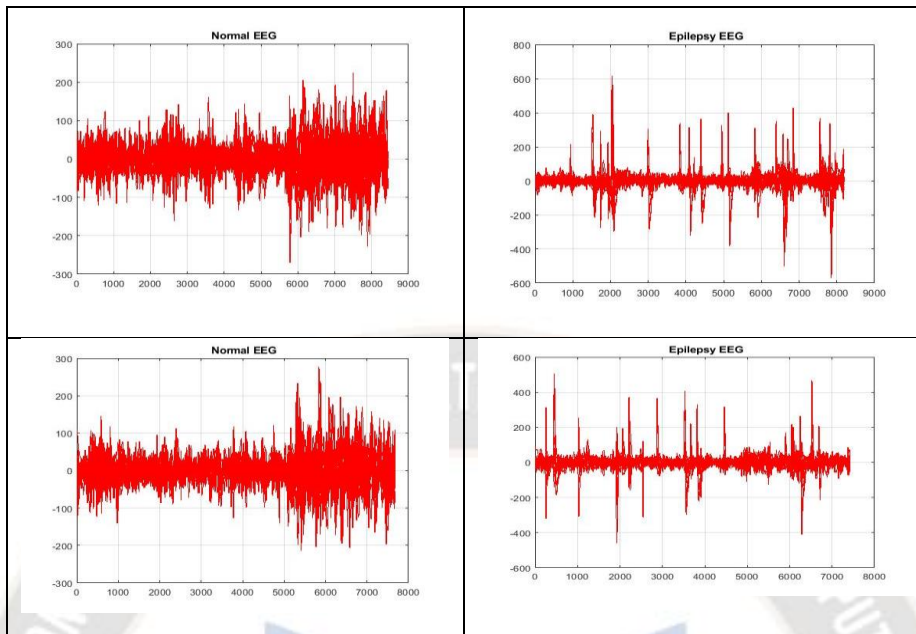


Figure 3. Representation of Normal EEG and EEG with Epilepsy

A. Accuracy

It is the ratio of incidence of epilepsy in the EEG signal is the total count of signal investigated. The value of accuracy is equated as Eq. (13)

$$Acy = \frac{True\ Positive + True\ Negative}{True\ Positive + True\ Negative + False\ Positive + False\ Negative} \quad (13)$$

Table 1. Analysis of Accuracy

Dataset	P-1D-CNN	S-CNN	TA-CNN-RNN	CGAN-TA-CNN-RNN
CHB-MIT-EEG	86.3	87.1	89.0	94.6
Bonn-iEEG	85.2	86.3	88.6	94.8
VIRGO-EEG	86.2	87.0	88.7	95.2

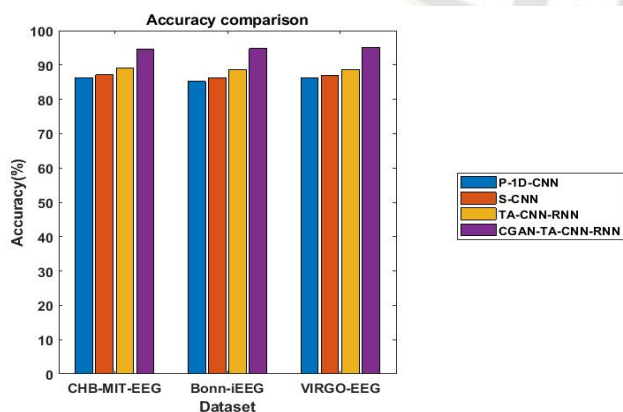


Figure 4. Accuracy vs. Different Datasets

Fig. 4 and Table 1 shows the accuracy achieved by the CGAN-TA-CNN-RNN is compared with the existing algorithms P-1D-CNN, S-CNN and TA-CNN-RNN. The accuracy of CGAN-TA-CNN-RNN is {9.62%, 8.61%, 6.29%} higher than the P-1D-CNN for {CHB-MIT-EG, Bonn-iEEG, VIRGO-EEG} correspondingly, {11.27%, 9.85%, 7%} higher than the S-CNN for {CHB-MIT-EG, Bonn-iEEG, VIRGO-EEG} correspondingly and {10.44%, 9.43%, 7.33%} higher than the TA-CNN-RNN for {CHB-MIT-EG, Bonn-iEEG, VIRGO-EEG} correspondingly. The realized maximum accuracy indicates the efficiency of the CGAN-TA-CNN-RNN technique.

B. Precision

True Positive (TP) and False Positive (FP) rates are used to calculate the precision. It is linearly proportional to the fraction of positive attributes in the entire EEG data Eq. (14)

$$Precision = \frac{True\ Positive}{True\ Positive + False\ Positive} \quad (14)$$

Table 2. Analysis of Precision

Dataset	P-1D-CNN	S-CNN	TA-CNN-RNN	CGAN-TA-CNN-RNN
CHB-MIT-EEG	84.7	85.9	88.3	93.9
Bonn-iEEG	84.2	85.1	87.7	94.5
VIRGO-EEG	86.4	87.2	89.4	94.9

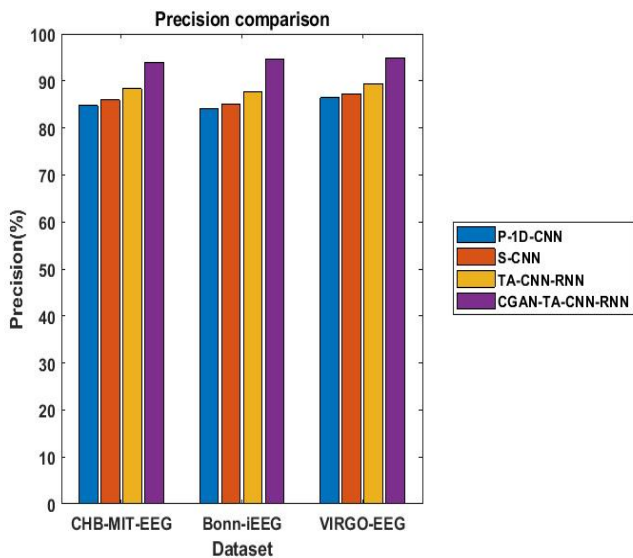


Figure 5. Precision vs. Different Datasets

Fig. 5 and Table 2 shows the precision achieved by the CGAN-TA-CNN-RNN is compared with the existing algorithms P-1D-CNN, S-CNN and TA-CNN-RNN. The precision of CGAN-TA-CNN-RNN is {10.86%, 9.31%, 6.34%} greater than the P-1D-CNN for {CHB-MIT-EG, Bonn-iEEG, VIRGO-EEG} correspondingly, {12.23%, 11.05%, 7.75%} greater than the S-CNN for {CHB-MIT-EG, Bonn-iEEG, VIRGO-EEG} correspondingly and {9.84%, 8.83%, 6.15%} greater than the TA-CNN-RNN for {CHB-MIT-EG, Bonn-iEEG, VIRGO-EEG} correspondingly. The attained maximum precision defines the efficiency of the CGAN-TA-CNN-RNN technique. shows the precision achieved by the CGAN-TA-CNN-RNN is compared with the existing algorithms P-1D-CNN, S-CNN and TA-CNN-RNN. The precision of CGAN-TA-CNN-RNN is {10.86%, 9.31%, 6.34%} greater than the P-1D-CNN for {CHB-MIT-EG, Bonn-iEEG, VIRGO-EEG} correspondingly, {12.23%, 11.05%, 7.75%} greater than the S-CNN for {CHB-MIT-EG, Bonn-iEEG, VIRGO-EEG} correspondingly and {9.84%, 8.83%, 6.15%} greater than the TA-CNN-RNN for {CHB-MIT-EG, Bonn-iEEG, VIRGO-EEG} correspondingly. The attained maximum precision defines the efficiency of the CGAN-TA-CNN-RNN technique.

C. Recall

It is measured depending on the epilepsy in the EEG signal identification at TP and False Negative (FN) values Eq. (15)

$$Recall = \frac{TP}{TP+FN} \tag{15}$$

Table 3. Analysis of Recall

Dataset	P-1D-CNN	S-CNN	TA-CNN-RNN	CGAN-TA-CNN-RNN
CHB-MIT-EEG	89.2	90.0	91.3	94.5
Bonn-iEEG	88.8	89.4	90.9	94.9
VIRGO-EEG	91.4	91.8	92.4	95.0

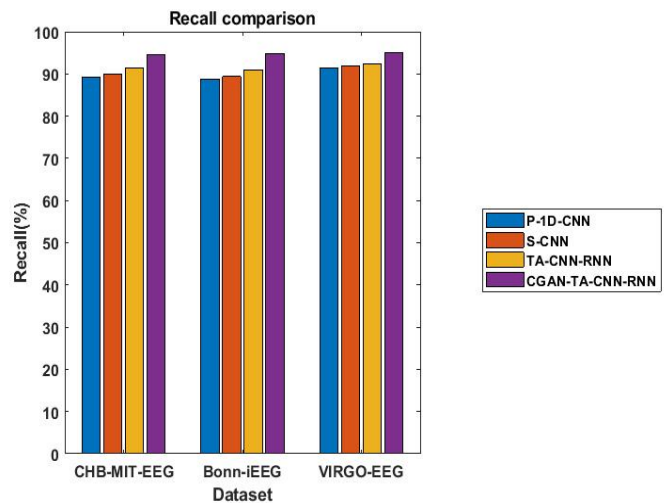


Figure 6. Recall vs. Different Datasets

Fig. 6 shows the recall achieved by the CGAN-TA-CNN-RNN is compared with the existing algorithms P-1D-CNN, S-CNN and TA-CNN-RNN. The recall of CGAN-TA-CNN-RNN is {5.94%, 5%, 3.5%} higher than the P-1D-CNN for {CHB-MIT-EG, Bonn-iEEG, VIRGO-EEG} correspondingly, {6.87%, 6.15%, 4.4%} higher than the S-CNN for {CHB-MIT-EG, Bonn-iEEG, VIRGO-EEG} correspondingly and {3.94%, 3.49%, 2.81%} higher than the TA-CNN-RNN for {CHB-MIT-EG, Bonn-iEEG, VIRGO-EEG} correspondingly. The attained maximum recall indicates the efficacy of the CGAN-TA-CNN-RNN.

D. F-Measures

It is determined by Eq. (16)

$$F - measure = \frac{2 \cdot Precision \cdot Recall}{Precision + Recall} \tag{16}$$

Table 4. Analysis of F-Measure

DATASET	P-1D-CNN	S-CNN	TA-CNN-RNN	CGAN-TA-CNN-RNN
CHB-MIT-EEG	86.9	88.0	89.8	94.2
BONN-iEEG	86.4	87.3	89.2	94.7
VIRGO-EEG	88.6	89.5	90.7	94.9

Fig. 7 shows and Table 4 shows the F-measure achieved by the CGAN-TA-CNN-RNN is compared with the existing algorithms P-1D-CNN, S-CNN and TA-CNN-RNN. The f-measure of CGAN-TA-CNN-RNN is {8.4%, 7.1%, 4.9%} higher than the P-1D-CNN for {CHB-MIT-EG, Bonn-iEEG, VIRGO-EEG} correspondingly, {9.61%, 8.48%, 6.17%} higher than the S-CNN for {CHB-MIT-EG, Bonn-iEEG, VIRGO-EEG} correspondingly and {7.11%, 6.03%, 4.63%} higher than the TA-CNN-RNN for {CHB-MIT-EG, Bonn-iEEG, VIRGO-EEG} correspondingly. The achieved maximum f-measure shows the efficiency of the CGAN-TA-CNN-RNN technique.

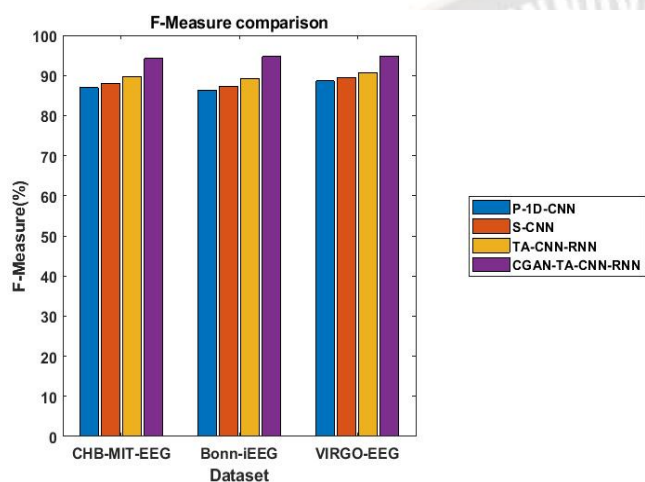


Figure 7. F-Measure vs. Different Datasets

## V. CONCLUSION

Epilepsy is a common cognitive illness that is characterized using involuntary periodic convulsions and it is detected with the EEG signals. EEG is the most utilised test to endorse cases of epilepsy. Generally, it has been demonstrated with possibly managing epilepsy without EEG. Attribute mining and pattern categorization are crucial in epilepsy prognosis. Because precise and useful attribute mining takes a long period to estimate, the typical usage of the sliding-window technique for constant EEG prognosis is limited in real-time. For an annotated huge dataset, a new regeneration model depending on the CGAN and a spatiotemporal error factor is proposed. The experimental results shows that the proposed CGAN- TA-CNN-RNN model attained classification accuracy of 94.6%, 94.8% and 95.2% on CHB-MIT-EEG, Bonn-iEEG and VIRGO-EEG which outperforms the existing technique. In future the approach can be extended to manage the huge signals with numerous channels.

## REFERENCES

[1] R. S. Fisher, W. V. E. Boas, W. Blume, C. Elger, P. Genton, P. Lee and J. Engel Jr, "Epileptic seizures and epilepsy: definitions proposed by the International League Against Epilepsy (ILAE) and the International Bureau for Epilepsy (IBE)," *Epilepsia*, vol.

46, no. 4, pp. 470-472, 2015, doi: 10.1111/j.0013-9580.2005.66104.x.

[2] H. Takahashi, S. Takahashi, R. Kanzaki and K. Kawai, "State-dependent precursors of seizures in correlation-based functional networks of electrocorticograms of patients with temporal lobe epilepsy," *Neurological Sciences*, vol. 33, no. 6, pp.1355-1364, 2012, doi: 10.1007/s10072-012-0949-5

[3] T. Zallas, M. G. Tsipouras, D. G. Tsalikakis, E. C. Karvounis, L. Astrakas, S., Konitsiotis and M. Tzaphlidou, "Automated epileptic seizure detection methods: a review study," *Epilepsy-histological, electroencephalographic and psychological aspects*, pp.75-98, 2012, doi: 10.5772/31597

[4] A. Sharmila, S. Aman Raj, P. Shashank and P. Mahalakshmi, "Epileptic seizure detection using DWT-based approximate entropy, Shannon entropy and support vector machine: a case study," *Journal of medical engineering & technology*, vol. 42, no. 1, pp. 1-8, 2018, doi: 10.1080/03091902.2017.1394389

[5] P. M. Shanir, K. A. Khan, Y. U. Khan, O. Farooq and H. Adeli, "Automatic seizure detection based on morphological features using one-dimensional local binary pattern on long-term EEG," *Clinical EEG and neuroscience*, vol. 49, no. 5, pp. 351-362, 2018, doi: 10.1177/1550059417744890.

[6] A. R. Hassan, and A. Subasi, "Automatic identification of epileptic seizures from EEG signals using linear programming boosting," *computer methods and programs in biomedicine*, vol. 136, pp. 65-77, 2016, doi:10.1016/j.cmpb.2016.08.013

[7] Y. S Park, G. R. Cosgrove, J. R. Madsen, E. N. Eskandar, L. R. Hochberg, S. S. Cash and W. Truccolo, "Early detection of human epileptic seizures based on intracortical microelectrode array signals," *IEEE Transactions on Biomedical Engineering*, vol. 67, no. 3, pp. 817-831, 2019, doi: 10.1109/TBME.2019.2921448.

[8] K. Belwafi, S. Gannouni and H. Aboalsamh, "An effective zero-time windowing strategy to detect sensorimotor rhythms related to motor imagery EEG signals," *IEEE Access*, vol. 8, pp. 152669-152679, 2020, doi: 10.1109/access.2020.3017888

[9] S. Chen, X. Zhang, L. Chen and Z. Yang, "Automatic diagnosis of epileptic seizure in electroencephalography signals using nonlinear dynamics features," *IEEE Access*, vol. 7, pp. 61046-61056, 2019, doi: 10.1109/ACCESS.2019.2915610

[10] M. C. Guerrero, J. S. Parada, and H. E. Espitia, "Principal Components Analysis of EEG Signals for Epileptic Patient Identification," *Computation*, vol. 9, no. 12, 133, 2021, doi: 10.3390/computation9120133.

[11] L. Hussain, "Detecting epileptic seizure with different feature extracting strategies using robust machine learning classification techniques by applying advance parameter optimization approach," *Cognitive neurodynamics*, vol. 12, no. 3, pp. 271-294, 2018, doi: 10.1007/s11571-018-9477-1.

[12] R. Sharma and R. B. Pachori, "Classification of epileptic seizures in EEG signals based on phase space representation of intrinsic mode functions," *Expert Systems with Applications*, vol. 42, no. 3, pp. 1106-1117, 2015, doi: 10.1016/j.eswa.2014.08.030.

[13] A. Malekzadeh, A. Zare, M. Yaghoobi, H. R. Kobravi and R. Alizadehsani, "Epileptic seizures detection in EEG signals using

- fusion handcrafted and deep learning features,” *Sensors*, vol. 21, no. 22, pp. 7710, 2021, doi: 10.1016/j.iot.2019.03.002.
- [14] R. M. Khati and R. Ingle, Feature extraction for epileptic seizure detection using machine learning. *Current medicine research and practice*, vol. 10, no. 6, pp. 266, 2020, doi: 10.4103/cmrrp.cmrrp\_52\_20.
- [15] H. T. Shiao, V. Cherkassky, J. Lee, B. Veber, E. E. Patterson, B. H. Brinkmann and G. A. Worrell, “SVM-based system for prediction of epileptic seizures from iEEG signal,” *IEEE Transactions on Biomedical Engineering*, vol. 64, no. 5, pp. 1011-1022, 2016, doi: 10.1109/tbme.2016.2586475.
- [16] Y. H. Liu, L. Chen, X. W. Li, Y. C. Wu, S. Liu, J. J. Wang, ..., and Y. Liu, “Epilepsy detection with artificial neural network based on as-fabricated neuromorphic chip platform,” *AIP Advances*, vol. 12, no. 3, pp. 035106, 2022, doi: 10.1063/5.0075761.
- [17] R. G. Thangarajoo, M. B. I. Reaz, G. Srivastava, F. Haque, S. H. M. Ali, A. A. A. Bakar and M. A. S. Bhuiyan, “Machine learning-based epileptic seizure detection methods using wavelet and EMD-based decomposition techniques: A review,” *Sensors*, vol. 21, no. 24, pp. 8485, 2021.
- [18] E. B. Assi, D. K. Nguyen, S. Rihana and M. Sawan, “Towards accurate prediction of epileptic seizures: A review,” *Biomedical Signal Processing and Control*, vol. 34, pp. 144-157, 2017, doi: 10.1016/j.bspc.2017.02.001.
- [19] A. Shoebi, M. Khodatars, N. Ghassemi, M. Jafari, P. Moridian, R. Alizadehsani, ..., and U. R. Acharya, “Epileptic seizures detection using deep learning techniques: A review,” *International Journal of Environmental Research and Public Health*, vol. 18, no. 11, pp. 5780, 2021, doi: 10.3390/ijerph18115780.
- [20] A. Abdelhameed and M. Bayoumi, “A deep learning approach for automatic seizure detection in children with epilepsy,” *Frontiers in Computational Neuroscience*, vol. 15, pp. 650050, doi: 10.3389/fncom.2021.650050.
- [21] S. T. Jaafar and M. Mohammadi, “Epileptic seizure detection using deep learning approach,” *UHD Journal of Science and Technology (UHDJST)*, vol. 3, no. 2, pp. 41-50, 2019, doi: 10.21928/uhdjst.v3n2y2019.pp41-50.
- [22] R. Hussein, H. Palangi, R. K. Ward and Z. J. Wang, “Optimized deep neural network architecture for robust detection of epileptic seizures using EEG signals,” *Clinical Neurophysiology*, vol. 130, no. 1, pp. 25-37, 2019, doi: 10.1016/j.clinph.2018.10.010.
- [23] N. A. Samee, N. F. Mahmoud, E. A. Aldhahri, A. Rafiq, M. S. A. Muthanna and I. Ahmad, “RNN and BiLSTM Fusion for Accurate Automatic Epileptic Seizure Diagnosis Using EEG Signals. *Life*, vol. 12, no. 12, pp. 1946, 2022, doi: 10.3390/life12121946.
- [24] M. Zhou, C. Tian, R. Cao, B. Wang, Y. Niu, T. Hu, ..., and J. Xiang, “Epileptic seizure detection based on EEG signals and CNN,” *Frontiers in neuroinformatics*, vol. 12, pp. 1-14, 2018, doi: 10.3389/fninf.2018.00095.
- [25] Irwansyah, E. ., Young, H. ., & Gunawan, A. A. S. . (2023). Multi Disaster Building Damage Assessment with Deep Learning using Satellite Imagery Data. *International Journal of Intelligent Systems and Applications in Engineering*, 11(1), 122–131. Retrieved from <https://ijisae.org/index.php/IJISAE/article/view/2450>.
- [26] P. Indurani and B. A. Firdaus Begam.” Prediction of Seizure in the EEG Signal with Time Aware Recurrent Neural Network,” *Revue d'Intelligence Artificielle*, vol. 36, no. 5, pp. 717-724, 2022, doi: 10.18280/ria.360508.
- [27] X. Yi, E. Walia and P. Babyn, “Generative adversarial network in medical imaging: A review,” *Medical image analysis*, vol. 58, pp. 101552, 2019, doi: 10.1016/j.media.2019.101552.
- [28] M. G. Bellemare and I. Danihelka, W. Dabney, S. Mohamed, B. Lakshminarayanan, S. Hoyer and R. Munos, “The cramer distance as a solution to biased wasserstein gradients,” *arXiv preprint arXiv:1705.10743*, May, 2017, <https://doi.org/10.48550/arXiv.1705.10743>
- [29] I. Ullah, M. Hussain, H. Aboalsamh, “An automated system for epilepsy detection using EEG brain signals based on deep learning approach”, *Expert Systems with Applications*, vol. 107, 2018, pp. 61-71, doi: 10.1016/j.eswa.2018.04.021
- [30] Ö. Türk and M. S. Özerdem, “Epilepsy detection by using scalogram based convolutional neural network from EEG signals,” *Brain sciences*, vol. 9, no. 5, pp. 115, May. 2019, doi: 10.3390/brainsci9050115.
- [31] F. Forooghifar, A. Aminifar and D. Atienza, “Resource-aware distributed epilepsy monitoring using self-awareness from edge to cloud,” *IEEE Transactions on Biomedical Circuits and Systems*, vol.13, no. 6, pp. 1338-1350, doi: 10.1109/TBCAS.2019.295122
- [32] R. Akut, “Wavelet based deep learning approach for epilepsy detection,” *Health information science and systems*, vol. 7, no. 1, pp. 1-9, 2019, doi: 10.1007/s13755-019-0069-1.
- [33] H. S. Chiang, M. Y., Chen and Y. J. Huang, “Wavelet-based EEG processing for epilepsy detection using fuzzy entropy and associative petri net,” *IEEE Access*, vol. 7, pp. 103255-103262, 2019, doi:10.1109/ACCESS.2019.2929266.
- [34] M. Sharma, S. Shahm and P. V. Achuth, “A novel approach for epilepsy detection using time–frequency localized bi-orthogonal wavelet filter,” *Journal of Mechanics in Medicine and Biology*, vol. 19, no. 01, pp. 1940007, 2019, doi.org/10.1142/S0219519419400074.
- [35] G. Andrzejak, K. Schindler, and C. Rummel, “Nonrandomness, nonlinear dependence, and nonstationarity of electroencephalographic recordings from epilepsy patients,” *Phys. Rev. E, Stat. Phys. Plasmas Fluids Relat. Interdiscip. Top.*, vol. 86, no. 4, pp. 046206, Oct. 2012, doi: 10.1103.
- [36] [http://epileptologiebonn.de/cms/upload/workgroup/lehnertz/eeg\\_data.html](http://epileptologiebonn.de/cms/upload/workgroup/lehnertz/eeg_data.html)
- [37] <https://iee-dataport.org/documents/eeg-datasetepileptic-seizure-patients#files>